Mechanical and Thermal Properties of High-Density Rigid Polyurethane Foams from Renewable Resources

M. Kirpluks[1]*, U. Cabulis[1], A. Ivdre[1], M. Kuranska[2], M. Zieleniewska[3], and M. Auguscik[3]

[1] *Latvian State Institute of Wood Chemistry, 27 Dzerbenes, LV-1006, Riga, Latvia*
[2] *Cracow University of Technology, Department of Chemistry and Technology of Polymers, 24 Warszawska, 31-155, Cracow, Poland*
[3] *Warsaw University of Technology, Faculty of Materials Science and Engineering, 141 Woloska, 02-507, Warsaw, Poland*

Received October 31, 2015; Accepted January 08, 2016

ABSTRACT: The most common sustainable solution for polyurethane (PU) materials is their production using renewable resources. Polyols derived from biomass and recycled polymers are the most promising way to do that. This study compares five different sustainable polyols as a possible raw material for production of high-density rigid PU foams for automotive application. The goal of our study was to show that biobased polyols are a suitable replacement for polyols derived from petrochemical products. The influence of the chemical structure of polyols on the PU polymer matrix and foam properties was investigated. Two sources of PU raw material feedstock were studied: the plant biomass and the side stream of poly(ethylene terephthalate) (PET) production. Three different polyols from renewable resources were investigated as well as two aromatic polyester polyols. High-density rigid polyurethane foams were developed from these raw materials. This was done to choose a material, which could be used as the core of structural elements for lightweight vehicles. The focus was put on the sustainability and competitive properties of the developed materials. The obtained results led to the conclusion that recycled PET polyols show a higher mechanical strength. Nevertheless, renewable resources are closely matched.

KEYWORDS: Renewable raw materials, rigid polyurethane foams

1 INTRODUCTION

Sustainable solutions have been studied across the whole range of polymer materials [1–4]. The focus has been put on polyurethane (PU) materials because at least one component of a polymer material can be obtained from renewable resources [1–10]. Recycled resources like the poly(ethylene terephthalate) (PET) manufacturing side stream can also be considered as a sustainable solution for polymer material production [11–13].

There is a broad range of applications for PU materials, such as flexible foams, rigid foams, thermoplastic elastomers, coatings and adhesives. Unfortunately, the majority of these materials are produced from petroleum-based feedstocks. In recent years, prices of crude oil and petroleum-based feedstocks have fluctuated significantly. Nonetheless, at the moment crude oil prices are the lowest in ten years [14], so it is important to find a suitable substitute for petrochemical materials, as they will eventually run out. Also, using renewable resources in polymer materials decreases the global warming potential of the material and have the potential to sequester a large amount of CO_2 from the atmosphere, while improving the impact the material has on the environment [15]. This has led to an increasing need and interest to develop alternate polyols (e.g., BASF castor oil-based Balance™, Cargill soybean-based BiOH™, Dow soybean-based Renuva™, etc.) based on renewable resource-based raw materials that offer reduced prices with a more favorable environmental footprint compared to current petroleum-derived polyols [16–18].

Renewable materials are usually introduced into the PU polymer matrix as a polyol component. Biobased polyols have been investigated for some time, and studies in this field are currently continuing. Good quality polyols have been obtained from different vegetable oils like rapeseed oil (RO), castor oil, palm oil and especially soybean oil [1–8]. Most of these oils are used already to produce a PU material feedstock on the industrial level [16–19].

**Corresponding author*: mkirpluks@gmail.com

DOI: 10.7569/JRM.2015.634132

© 2016 Scrivener Publishing LLC

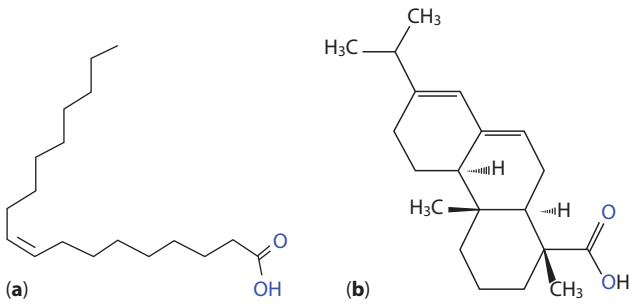

Figure 1 Basic structure of TO components: a) fatty acid (oleic acid); b) rosin acid (abietic acid).

Industry uses renewable raw materials not only because of the sustainability and marketing aspect of the products. These materials provide a competitive and commercially viable alternative to petrochemical resources [19]. Vegetable oil polyols also provide additional positive properties of a PU material, like higher hydrophobicity [10].

Unfortunately, most of the mentioned vegetable oils can be classified as first generation biobased raw materials [20–21]. This means that the production of these polyols is competing with the production of food. Tall oil (TO) can tackle this problem as it is a byproduct of cellulose production—a product of forest biomass processing and not an agricultural product. TO is a mixture of fatty and rosin acids, the generic structures of which can be seen from Figure 1 [22–25]. TO should be chemically modified by the introduction of two or more hydroxyl groups in order to use it as a raw material for production of PU.

A renewable polyol from TO was synthesized at the Latvian State Institute of Wood Chemistry (IWC) by the esterification method with triethanolamine (TEOA). Distilled TO with 20% rosin acid content from Forchem (Finland) was used as a raw material. Figure 2 shows the TO esterification with TEOA [22, 23].

In this study, RO was used as the second renewable material feedstock. Polyols for rigid PU foam production were obtained by two synthesis methods. RO polyol was synthesized similarly to TO polyol by transesterification of triglyceride structure of RO with TEOA. The third type of biobased polyol was also obtained from RO but double bonds in the RO chemical structure were targeted to introduce hydroxyl groups into the compound [8].

Another way to replace petrochemical resources in PU foams is to use recycled materials. The PET manufacturing side stream provides an ideal resource for aromatic polyester polyols [APP]. PU foams obtained from these polyols have better mechanical and thermal properties because of the introduction of the aromatic structure into the PU polymer matrix [12, 13]. Generic

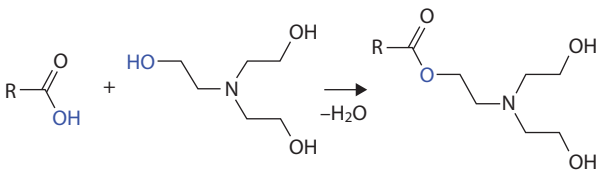

Figure 2 Reaction scheme of TO esterification with TEOA [22, 23].

glycolysis of PET with diethylene glycol (DEG) can be seen from Figure 3.

Another component, polyisocyanate, is not yet produced from renewable resources on the industrial scale. Nevertheless, this topic is also investigated even if it is much more difficult than the synthesis of "green" polyols. Nonrenewable polyisocyanate is the reason why it is possible to obtain only 20–35% of the renewable material content in PU materials on the industrial scale.

PU materials have a very wide range of properties, which is the main reason why they are used in almost every aspect of modern life. Previous studies have been focused on rigid PU foams, which are used mainly as a thermal insulation material in the construction industry and in the global appliances (refrigerators, freezers, etc.) industry. A general review of the PUR industry and the physics of heat transfer in cellular materials can be found [3, 19, 26, 27]. The density of rigid PU foam thermal insulation usually ranges from 40 to 60 kg/m^3. the present study investigates high-density (200 kg/m^3) rigid PU foams that are used as thermal insulation at cryogenic temperatures [28]. With increasing density of rigid PU foams, mechanical strength also increases [29]; therefore, the developed material at a density of 200 kg/m^3 would be strong enough to use as the core of structural elements.

The main objective of this research was to choose a material that would be used as a structural foam material for lightweight vehicles. The focus was put on the sustainability and competitive properties of the developed materials.

2 EXPERIMENTAL

2.1 Materials and Polyol Properties

The most significant properties of the polyols used in this study are presented in Table 1. TO polyol and RO polyols were synthesized at IWC [9, 22, 23]. Epoxidized RO polyol was synthesized at the Cracow Technical University [9, 10, 30].

The APPs used in this study were produced by Neo Group, Lithuania. The main business of this company

© 2016 Scrivener Publishing LLC

 DOI: 10.7569/JRM.2015.634132

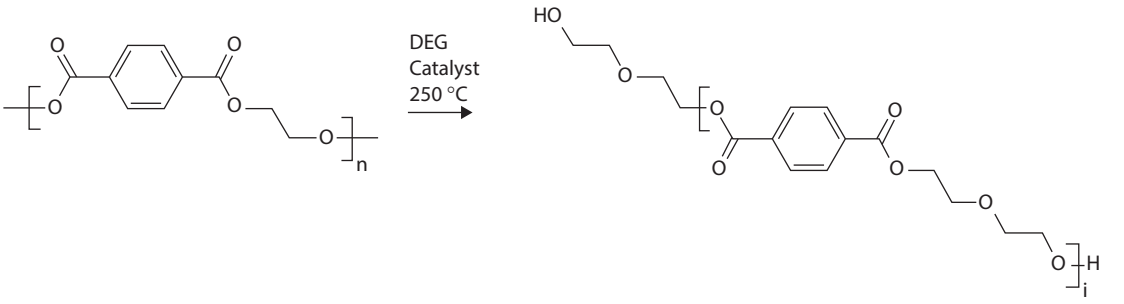

Figure 3 Glycolysis of PET [12, 13].

Table 1 Technical data of polyols obtained from sustainable resources.

Polyol type		OH value, mgKOH/g	Viscosity at 25°C, mPa·s	Acid value, mgKOH/g	M_n, g/mol	f_n	Water content, %
Renewable polyols	TO polyol	342	280 ± 25	< 5	391	2.39	0.24
	RO polyol	301	190 ± 25	< 5	474	2.55	0.05
	RO Epoxy	276	2260 ± 50	< 5	635	3.12	0.36
Recycled polyols	Neopolyol 240 (NEO 240)	258	5000 ± 500	< 5	683	3.14	0.04
	Neopolyol 380 (NEO 380)	366	3500 ± 500	< 5	505	3.30	0.12

is the production of PET granules and PET bottles. The side stream of those commodities contains PET dust and other industrial waste, which is directly transferred into a glycolysis reactor where it is converted into APP. Glycolysis of the PET side stream is done by using DEG. Changing the technical parameters and the catalyst amount, two different grades of APPs are produced [31].

Gel permeation chromatography was used to determine the values of the number-average molecular weight (M_n) and number-average functionality (f_n) of the obtained polyols. The number-average functionalities of polyols were calculated based on hydroxyl values, and number-average molecular weight was experimentally determined (Equation 1) [9].

$$f_n = \frac{M_n \cdot OH_{val}}{56110} \quad (1)$$

where f_n is the number-average functionality; M_n is the number-average molecular weight; and OH_{val} is the hydroxyl value of polyol.

Viscosity of polyols was determined according to DIN 53015 standard at 25 °C using a Falling Ball Viscometer KF 100 from Rheo Tec Messtechnik GmbH Germany. Water content of polyols was determined according to DIN 51777 standard.

The chemical structure of the used polyols was studied by Fourier transform infrared spectroscopy (FTIR) measurements. Figure 4 presents FTIR spectra of polyols from renewable materials, and Figure 5 shows FTIR spectra of polyols from recycled raw materials. Peaks at 3444–3385 cm^{-1} indicated the presence of OH groups in the polyols chosen for this project. TO polyol and RO polyol showed double bond stretching at 3008 cm^{-1}. In contrast, RO Epoxy polyol did not have this peak as double bond was transformed in the epoxidation and ring-opening reaction. TO and RO polyol FTIR spectra were quite similar as expected, which was also due to the similarity of the chemical structure. The tertiary amine groups' vibrations are seen at 1043–1042 cm^{-1}. the RO Epoxy polyol differs from the TO and RO polyols with ether bond –C-O-C- symmetric stretching at 1103 cm^{-1}, which is present due to epoxy ring opening with diethanolglycol. The lack of epoxy ring vibration at the 928 cm^{-1} peak confirms the ring-opening reaction. Addition of tertiary amine groups into the polyol could make it more catalytically active, as most commercial PU catalysts are amine based. This could be a beneficial property because catalysts are among the most expensive components in PU foam formulation. The TO polyol should contain aromatic structures because distilled TO with 20% of rosin acids was used to synthesize the TO polyol. Unfortunately, no aromatic structures were detected in FTIR spectra in contrast to the case of APP polyols, which had aromatic group signals at 1410 cm^{-1} and 734 cm^{-1}. Also, the aromatic acid ester signal at 1282 cm^{-1} is related to the presence of an

 © 2016 Scrivener Publishing LLC

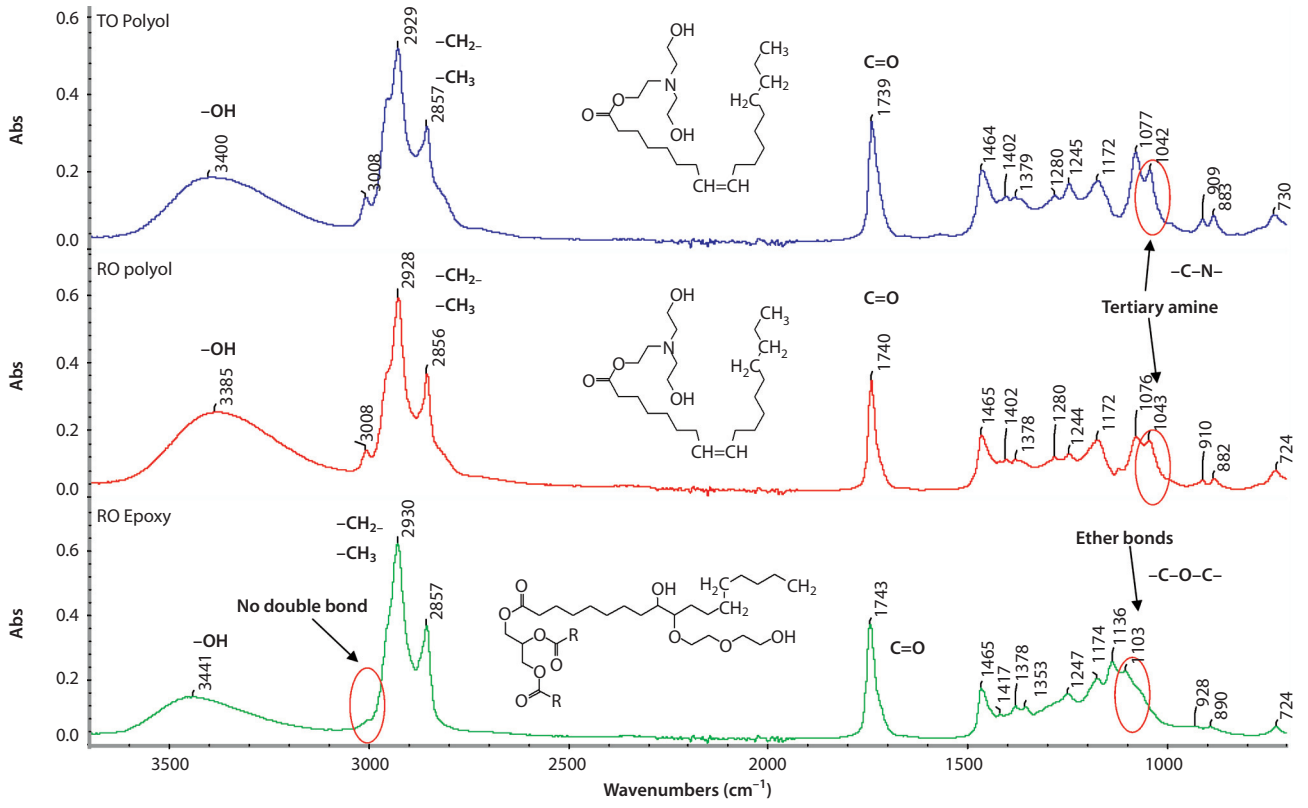

Figure 4 FTIR spectra for polyols from renewable raw materials.

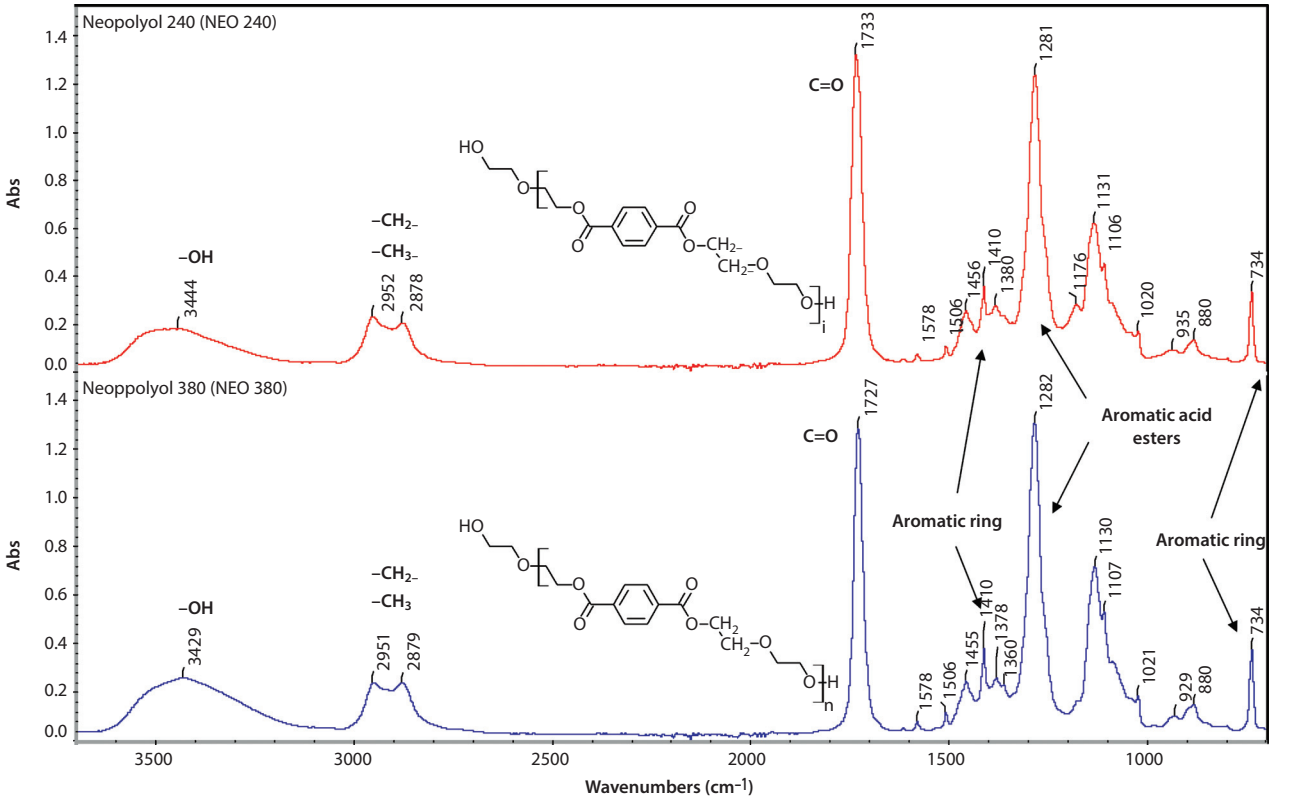

Figure 5 FTIR spectra for polyols from recycled PET.

© 2016 Scrivener Publishing LLC

aromatic ring in APP polyols. The difference between renewable and recycled polyols can be seen at ~2930 and ~2860 cm^{-1} of C-H symmetric and asymmetric stretching. For APP, this signal is almost not present, showing less aliphatic chains in polyols. All polyols showed a C=O bond stretching peak at 1760–1665 cm^{-1} [9, 32, 33].

Polyols from renewable and recycled resources were used as the base of high-density PU foam formulation. Higher functional polyether polyol based on sorbitol Lupranol 3422 (contains only secondary hydroxyl groups, OH value 490 mg KOH/g) from BASF was added to increase the cross-linkage density of the polymer matrix. An additive surfactant NIAX Silicone L6915 was used to obtain closed-cell PU foams. The reactive delayed action time amine-based catalyst NP-10, available from Momentive Performance Materials Inc., was used. Tris(chloropropyl)phosphate (TCPP) from LANXESS Deutschland GmbH was used as a flame retardant. Distilled water was used as a chemical blowing agent. Polymeric diphenylmethane diisocyanate – IsoPMDI 92140 (pMDI) from BASF – was used as an isocyanate component (NCO = 31.5 wt%).

2.2 PUR Foam Sample Preparation

The polyol component was obtained by weighting all necessary components (all polyols, the catalyst, blowing agent, surfactant and flame retardant) presented in Table 2 and stirring them for 1 min by a mechanical stirrer at 2000 rpm. PU foams were prepared after conditioning the polyol system at room temperature for at least 2 h in a sealed container to remove the air mixed in.

Isocyanate pMDI and the polyol component were weighted and mixed by a mechanical stirrer at 2000 rpm for 15 sec to prepare PU foams. For the isocyanate index, the ratio of the equivalent amount of isocyanate used relative to the theoretical equivalent amount times 100, 160 was chosen for all PU foams. Then, the reacting mixture was poured into a stainless steel mold that was preheated to 50 °C and placed on a balance. An appropriate amount of the reacting PU mass was poured into the mold and then the mold was sealed. The lid of the mold was kept in place by four steel eye bolts with M12 thread, which are embedded into the bottom lid of the mold. The mass of the reacting mixture was chosen to obtain PU foams with an approximate density of 200 kg/m^3. The air was able to escape from the mold through the opening on the top of the mold's lid, which was closed after all air escaped. After that, PU foams were cured at 50 °C for 2 h. At that point, the mold was cooled to room temperature and PU foams were removed and conditioned for at least 24 h. Then, the samples for tests were cut out according to the respective standards. The samples were cut from the inner part of the PU foam block at least 10 mm from the PU foam block walls. This insured that integral skin of PU foam block did not have an effect on sample properties. Samples were prepared in a stainless steel mold to keep the same apparent density across all the samples. The PU

Table 2 Polyol formulation, renewable material content in PU foams, technological parameters, apparent density and closed cell content of PU foams.

Polyol formulation	**TO polyol**	**RO polyol**	**RO epoxy**	**NEO 240**	**NEO 380**
Green Polyol, pbw	80.0				
Cross linkage reagent (Lupranol 3422)	20.0				
Flame retardant (TCPP)	20.0				
Blowing reagent (water)	1.0				
Reactive catalyst	0.3	0.3	1.6	1.6	1.6
Surfactant	2.0				
Polyisocyanate (pMDI)	179.7	176.5	160.0	156.0	188.9
Isocyanate index	160	160	160	160	160
Characteristics of system					
Renewable materials in polyurethane foam, %	17.9	18.1	19.1	13.7	14.3
Technological parameters					
Start time, s	50	25	34	27	25
String time, s	115	50	80	45	45
Tack free time, s	180	80	160	58	60
End time, s	120	95	120	60	60
Apparent density of molded PU foams, kg/m^3	202.6 ± 1.0	203.3 ± 2.2	203.1 ± 1.3	207.8 ± 1.2	209.6 ± 1.2

© 2016 Scrivener Publishing LLC

foam block dimensions and generic sample placement in PU foam block are shown in Figure 6.

Renewable materials' content was calculated based on the mass of renewable materials used in PU foam formulation. *Stoichiometric* ratios of TO, rapeseed oil and PET in polyols, as well as the sorbitol content in Lupranol 3422, were taken into account.

2.3 PUR Characterization Methods

The physical and mechanical properties of the foams were measured in accordance with the following standards: foam density – ISO 845; compression strength – ISO 844; tensile strength – ISO 1926, Poisson's ratio was measured using a video extensometer; closed-cell content – ISO 4590. The compression strength of PUR was tested parallel and perpendicular to foam rise with one offset from ISO 844 standard – sample size; cylinders with a diameter of 20 mm and a height of 22 mm were tested. Mechanical testing of PUR was performed on Zwick/Roell 1000 N (Ulm, Germany) testing machines.

A Tescan TS 5136 MM scanning electron microscope (SEM) with a secondary electron (SE) detector was used to take images of surface morphology. Before the SEM investigation, samples with a size of 1 × 1 × 0.2 cm were cut and sputtered with a gold layer using an Emitech K550X sputter coater (current 25 mA, coating time 2 min). Obtained data and images were processed with Vega TC software.

To clarify the shape, average size of cells, cell size distribution and anisotropy coefficient, images were taken in parallel and perpendicular directions to foam rise. Cells in cross-section images were measured both lengthwise and breadthwise. For each sample, more than 200 cells were measured. To determine cell size distribution, the number of cells in the 20 µm interval was divided by the total number of cells. Anisotropy coefficient was calculated using Equation 2.

$$R = \frac{\sum_{i=1}^{n} \frac{h}{l}}{n} \quad (2)$$

where h – cell size lengthwise; l – cell size breadthwise; n – total number of cells.

The SEM images were analyzed by ImageJ software. Using this software, the cell density (N_f) was

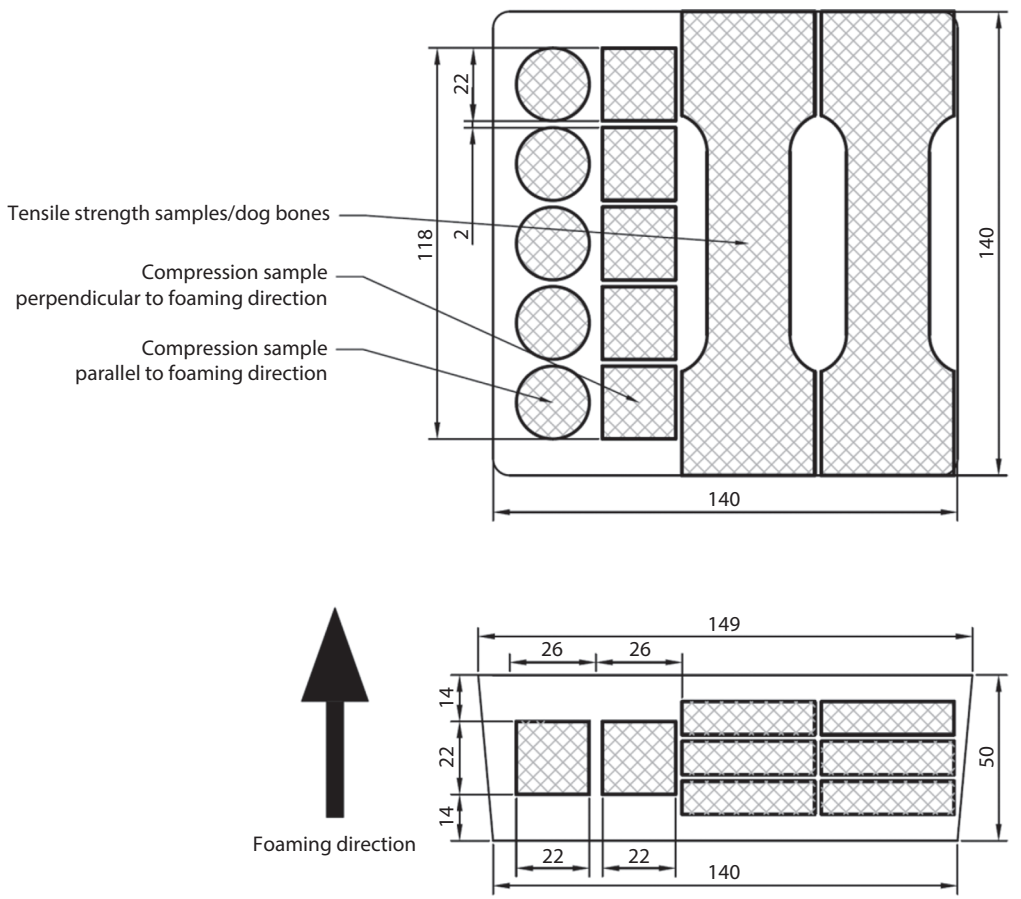

Figure 6 PU foam block obtained from stainless steel mold and mechanical properties sample placement.

© 2016 Scrivener Publishing LLC

determined by the number of cells per unit volume of foam, which was calculated using Equation 3 [34].

$$N_f - \left(\frac{n \cdot M^2}{A}\right)^{3/2} \quad (3)$$

where n – the number of cells in the micrograph; M – the magnification of the micrograph; A – the area of the micrograph (cm^2).

FTIR spectroscopy data were used to monitor the functional groups of the synthesized products; the chemical constitution of the developed rigid PU foams and degree of phase separation were determined using the infrared spectra obtained with a Nicolet 6700 (Thermo Electron Corp.) spectrometer with an attenuated total reflection (ATR, resolution 4 cm^{-1}). 2 mm thick rigid PU foam samples were cut from the middle of the foam block and scanned 64 times in the 4000–400 cm^{-1} range. Data processing was performed using OMNIC Spectra 2.0 software (Thermo Fisher Scientific Inc, UK).

FTIR absorption spectra of the stretching vibrations of the –C=O group in the range of 1760–1650 cm^{-1} were analyzed. The intensity of individual signals was determined with a split of the multiplet peak of the carbonyl band via Gaussian curve fitting using OMNIC Spectra 2.0 software. The degree of the carbonyl groups participating in hydrogen bonding can be described by the carbonyl hydrogen bonding index, $R_{C=O}$, as given in Equation 4. On the basis of the intensity of the peaks, $R_{C=O}$ index was calculated, defining the participation of urethane and urea groups forming hard segments, linked with the hydrogen bond of –C=O groups [35, 36].

$$R_{C=0} = \frac{A_{B1} + A_{B2}}{A_{F1} + A_{F2}} \quad (4)$$

where A_{B1}, A_{B2} are the respective surface areas of peaks from vibrations bound with the hydrogen bond of the carbonyl groups of urea (*B*1) and urethane (*B*2) bonding; and A_{F1}, A_{F2} are the respective surface areas of peaks from vibrations unbounded with the hydrogen bond of the carbonyl groups of urea (*F*1) and urethane (*F*2) bonding.

Moreover, the degree of phase separation (*DPS*) was obtained from Equation 5.

$$DPS = \frac{R_{C=0}}{1 + R_{C=0}} \quad (5)$$

The changes in carbonyl hydrogen bonding and in *DPS* affect the properties of PUs, as presented in the work by Pretsch *et al.* [37], as well as Ryszkowska *et al.* [35, 39].

With the use of the results of multiplet band distribution, the participation of urethane bonds (U_1), urea bonds (U_2) and allophanate bonds (A_L) in hard segments was also calculated by means of the formulae below:

$$U_1 = \frac{\sum A_{1i}}{\sum A_i} \quad (6)$$

$$U_2 = \frac{\sum A_{2i}}{\sum A_i} \quad (7)$$

$$U_3 = \frac{\sum A_{3i}}{\sum A_i} \quad (8)$$

where: U_1, U_2, A_L are contributions of urethane (1), urea (2) and allophanate groups (3); A_{1i}, A_{2i}, A_{3i} are absorbance of carbonyl groups of urethane (1), urea (2) and allophanate groups (3), respectively, and A_i is the absorbance of carbonyl groups in the 1760 cm^{-1} and 1650 cm^{-1} region from carbonyl in the hard segment.

Dynamic mechanical analysis (DMA) was carried out to determine the glass transition temperature of PU foams. DMA analysis was done using Mettler Toledo DMA/SDTA 861e equipment in the three-point bending regime for PU foam samples with dimensions of 30 × 12 × 4 mm. DMA samples were cut from the inner part of the PU foam block using a band saw. Their surface was ground using an industrial abrasive, and afterwards dust was removed with a high pressure blower. DMA was performed using a constant frequency of 1 Hz and an amplitude of 20 µm. A heating rate of 3 °C/min and a temperature range between –50 and 200 °C were also used. The glass transition temperature (T_g) from DMA analysis was considered as a peak point of tan (δ).

Thermal degradation of PU foams was analyzed by thermogravimetric analysis (TGA). Foam samples of 10 ± 1 mg were placed on platinum scale pans and heated in an air atmosphere at 10 °C/min at a temperature range of 25–1000 °C. Data processing was performed using OriginPro 8.5.1 and TA Instruments' Universal Analysis 2000 v4.5A software.

3 RESULTS AND DISCUSSION

3.1 Morphological Analysis of Developed PU Foams from Different Polyols

SEM was used to obtain images of the developed rigid PU foams from which average cell length, width and anisotropy index were determined (Table 3). It can be seen that the polyol type did not influence the isotropic properties of the PU foams. The average anisotropy coefficient across all types of rigid PU foams was 0.99 ± 0.04. But there was noticeable difference in cell density of PU foams where Neo 380 polyol had the

© 2016 Scrivener Publishing LLC

highest value. The SEM images of the developed rigid PU foams from renewable and recycled resources and their cell size distribution histograms are shown in Figure 7. It can be seen that foams from RO/TEOA polyol had the largest cells as well as the most broad/uneven cell size distribution, which correlated with the smallest cell density.

As compared to PU foams from renewable resources, PU foams from recycled resources (APP, Neo 380) showed a smaller cell size and a more uniform cell size distribution (Figure 7). When two APP polyols were compared with each other, Neo 380 gave more desirable cell morphology.

3.2 Mechanical Properties of PU Foams

Compression, tensile and impact strength tests were done for PU foams from six sustainable polyols with an apparent density of 200 ± 10 kg/m^3. Compression strength was measured in directions parallel and perpendicular to foam rise to confirm the isotropic properties of the developed materials. It should be

Table 3 Cell dimensions and coefficient of anisotropy for obtained PU foams from five different polyols.

Polyol type	Cell length, μm	Cell width, μm	Anisotropy coefficient	Cell density, cells/cm^3 ·10^{12}
TO polyol	158 ±33	165 ±34	0.96 ±0.02	1.360
RO polyol	252 ±42	268 ±45	0.94 ±0.02	0.323
RO epoxy polyol	179 ±31	171 ±27	1.05 ±0.03	0.836
NEO 240	155 ±23	153 ±21	1.01 ±0.02	1.550
NEO 380	123 ±21	123 ±21	1.00 ±0.02	5.180

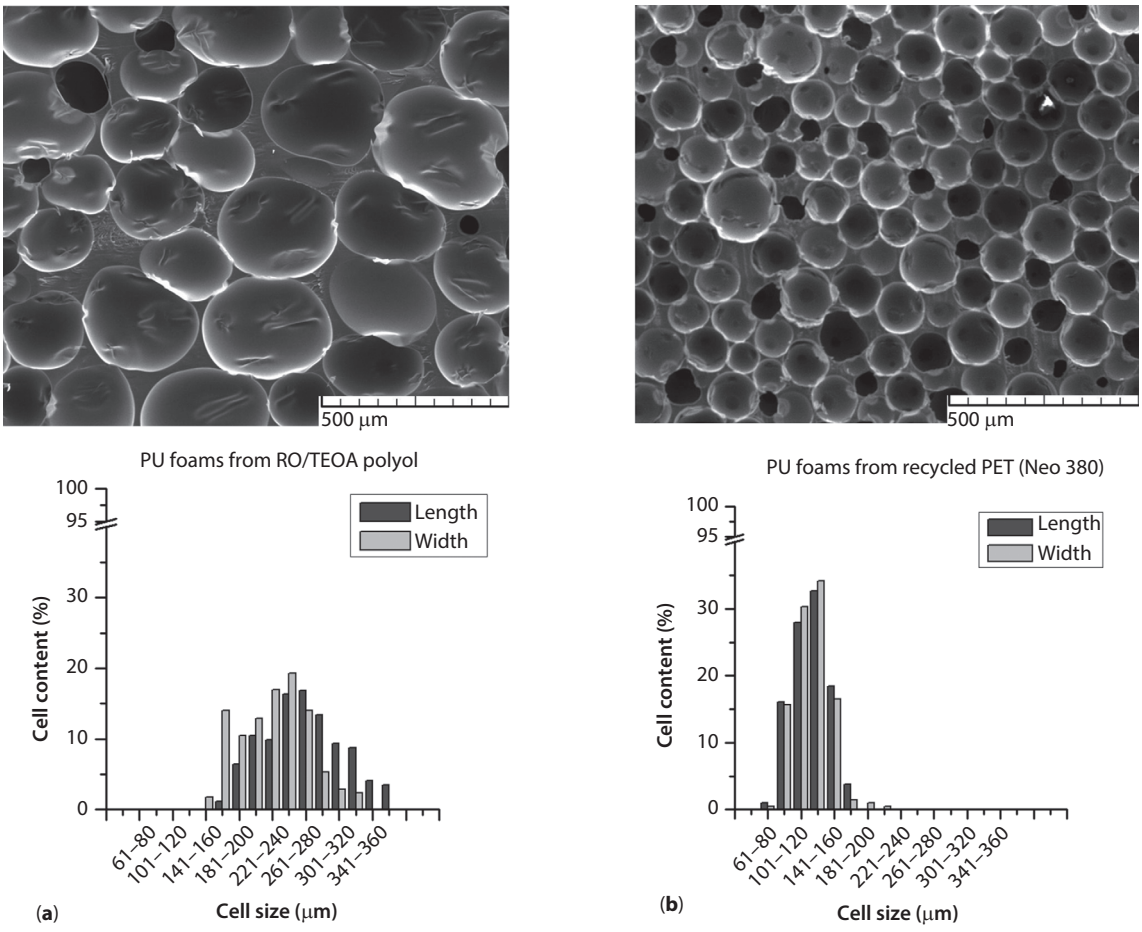

Figure 7 SEM images of rigid PU foams from (**a**) RO/TEOA polyol and (**b**) recycled PET (Neo 380).

© 2016 Scrivener Publishing LLC

noted that the anisotropy of the foamed material is more dependent on the foam production method and the mold design than on the material formulation. Compression strength and Young's modulus of the developed PU foams with an apparent density of 200 ± 10 kg/m^3 are shown in Table 4.

As might be expected, compression tests showed that the mechanical properties of PU foams are enhanced by introducing aromatic structure polyols into the PU polymer matrix. It is especially noticeable in the results of Young's modulus where both PET polyols showed about 20% higher compression strength values. The most even cell size distribution of PU foams (anisotropy coefficient = 1,00) obtained from Neo 380 polyol contributed to small differences between compression strength and Young's modulus when testing force is applied parallel and perpendicular in regard to the PU foaming direction. The lowest quality foams were obtained from the RO/TEOA polyol. After sample preparation, it was noticed that on the bottom of the container of RO/TEOA polyol there was a clearly separate phase of unknown residue. Most likely the synthesized polyol is not stable and the transesterification reaction is retrogressive. This can influence the PU foam polymer matrix because of the higher amount of monofunctional diglycerides, which can stop the polycondensation reaction, thus reducing the overall length of polymer chains. The phase separation of RO/TEAO polyol will be investigated further but it is clear that this polyol is not yet ready for any kind of up-scaling. In tensile strength tests, PU foams from PET showed a similar result to compression tests with higher Young's modulus and only slightly higher tensile strength values (Table 4). The Poisson's ratio was similar to all types of polyols.

3.3 Thermal Stability of PU Foams

The TGA analysis data for the developed PU foams are presented in Table 5. Figures 8 and 9 demonstrate TGA graphs for PU foams from renewable and recycled polyols, respectively. The first initial step of mass loss (T_1 and $T_{5\%}$) can be attributed to the release of the additive flame retardant TCPP, unreacted isocyanate/polyols, water moisture and other small volatiles. Hence, the peak of this mass loss is not clearly seen; it was determined using the multiple Gaussian peak fit tool in OriginPro software. For PU foams obtained from the RO epoxy polyol, this first step of degradation was at a higher temperature, which suggests a more crosslinked structure of the polymer. Also, the RO epoxy polyol showed a higher thermal stability, compared to TO and RO polyols. The next stage of degradation at T_2 245–255 °C is related to the oxidative degradation of PU soft segments, and in

Table 4 Compression and tensile properties of rigid PU foam from renewable and recycled polyols.

Compression properties				
	Young's modulus		Compression strength	
	Perpendicular to foaming direction	Parallel to foaming direction	Perpendicular to foaming direction	Parallel to foaming direction
	MPa	MPa	MPa	MPa
Polyol type	67.3 ±1.3	64.7 ±0.7	2.55 ±0.01	2.36 ±0.03
TO polyol	52.7 ±3.0	50.4 ±2.1	2.23 ±0.09	1.97 ±0.03
RO polyol	66.7 ±1.9	66.4 ±0.7	2.46 ±0.05	2.38 ±0.03
RO Epox	82.1 ±9.4	67.8 ±6.6	2.79 ±0.19	2.66 ±0.02
NEO 240	78.7 ±3.9	81.7 ±1.1	2.80 ±0.04	2.72 ±0.05
NEO 380	67.4 ±1.3	64.7 ±0.7	2.55 ±0.01	2.36 ±0.03

Tensile properties					
	Apparent density	Young's modulus	Tensile strength	Elongation at break	Poisson's ratio
Polyol type	kg/m^3	MPa	MPa	%	
TO polyol	202.6 ±1.0	114.7 ±4.7	2.93 ±0.02	5.1 ±0.2	0.44 ±0.21
RO polyol	203.3 ±2.2	94.0 ±0.5	2.45 ±0.10	4.8 ±0.4	0.37 ±0.08
RO Epox	203.1 ±1.3	102.1 ±17.5	2.66 ±0.05	4.6 ±0.3	0.33 ±0.06
NEO 240	207.8 ±1.2	136.7 ±3.1	3.15 ±0.06	7.4 ±0.4	0.33 ±0.03
NEO 380	209.6 ±1.2	129.0 ±3.6	2.99 ±0.17	4.2 ±1.0	0.31 ±0.06

© 2016 Scrivener Publishing LLC

Table 5 Thermal stability properties for rigid PU foams, temperatures of different stages of PU foam degradation [°C].

Polyol type	T_{onset}	$T_{5\%}$	$T_{25\%}$	$T_{50\%}$	T_1	T_2	T_3	T_4	T_5
TO polyol	143	191	281	479	182	253	273	446	544
RO polyol	151	201	297	474	187	253	280	439	545
RO epoxy polyol	146	195	311	463	200	–	302	456	548
NEO 240	150	203	289	485	181	248	280	433	544
NEO 380	148	196	310	511	176	–	300	–	543

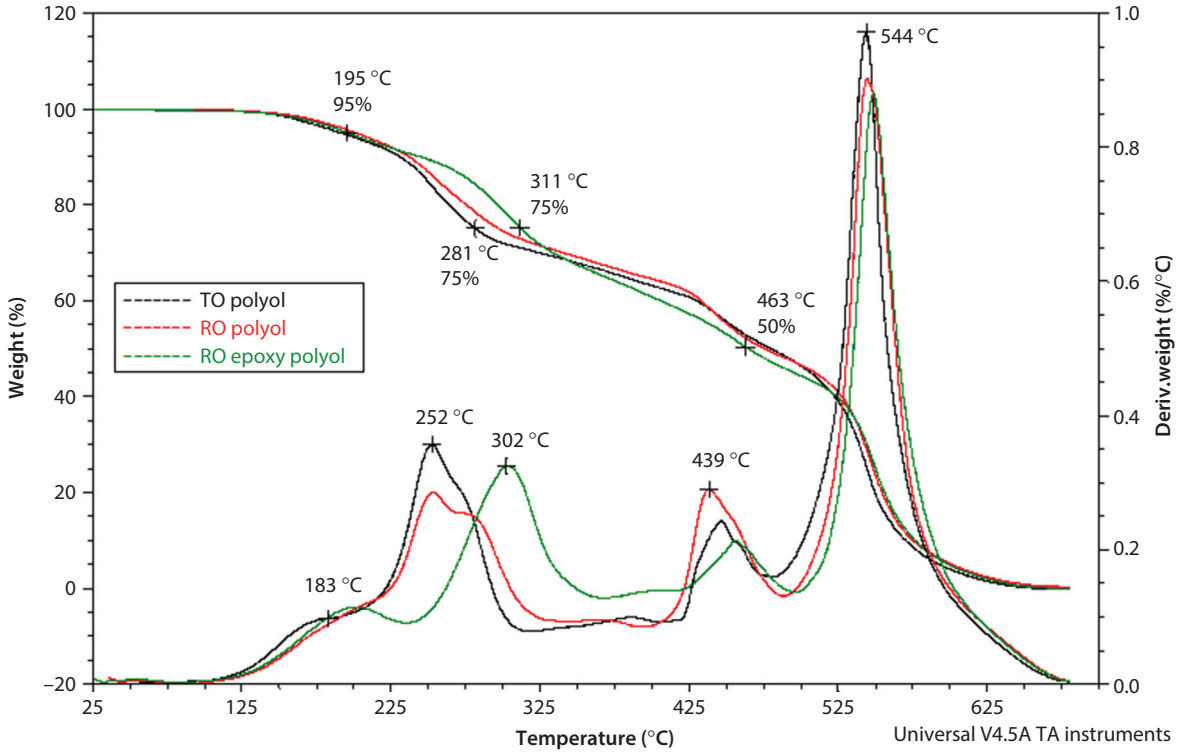

Figure 8 TGA curves for PU foams from TO, RO and RO Epoxy polyols.

the case of TO and RO polyols, decoupling and oxidation of fatty acid dangling chains [40, 41]. For TO, RO and Neo 240 polyols, there is the second step of soft segment degradation at T_3 273–280 °C. For RO epoxy polyols and Neo 380, the degradation process of soft segments is at higher temperatures T_3 – 300°C, which confirms the more crosslinked structure of the polymer. The Neo 240 PET polyol showed a significantly lower thermal stability than the Neo 380 PET polyol with a higher OH value. Shorter PET polyol chains of Neo 380 are attributed to the higher content of hard segments, which are more thermally stable [41]. T_4 at 430–450 °C represents the degradation and oxidation of the isocyanate and aromatic part of PU foams and T_5 at 540–545 °C is the oxidation of char and aromatics.

3.4 Glass Transition Temperature of PU Foams

The T_g was determined by DMA analysis of the PU foam material, and the results are presented in Figure 10. DMA graphs (Figure 10) show that the storage modulus of PU foams from PET polyols is higher than that for PU foams from renewable polyols. Also, the PU foams from renewable polyols had much less repeatable results due to the less homogeneous structure of polyols. As expected, higher cross of PU foams from the Neo 380 polyol delivered higher T_g, compared to the Neo 240 polyol. The overall conclusion is that all developed PU foams except Neo 240 have very close T_g ~134–145 °C. This means that these materials should not lose their mechanical

© 2016 Scrivener Publishing LLC

 DOI: 10.7569/JRM.2015.634132

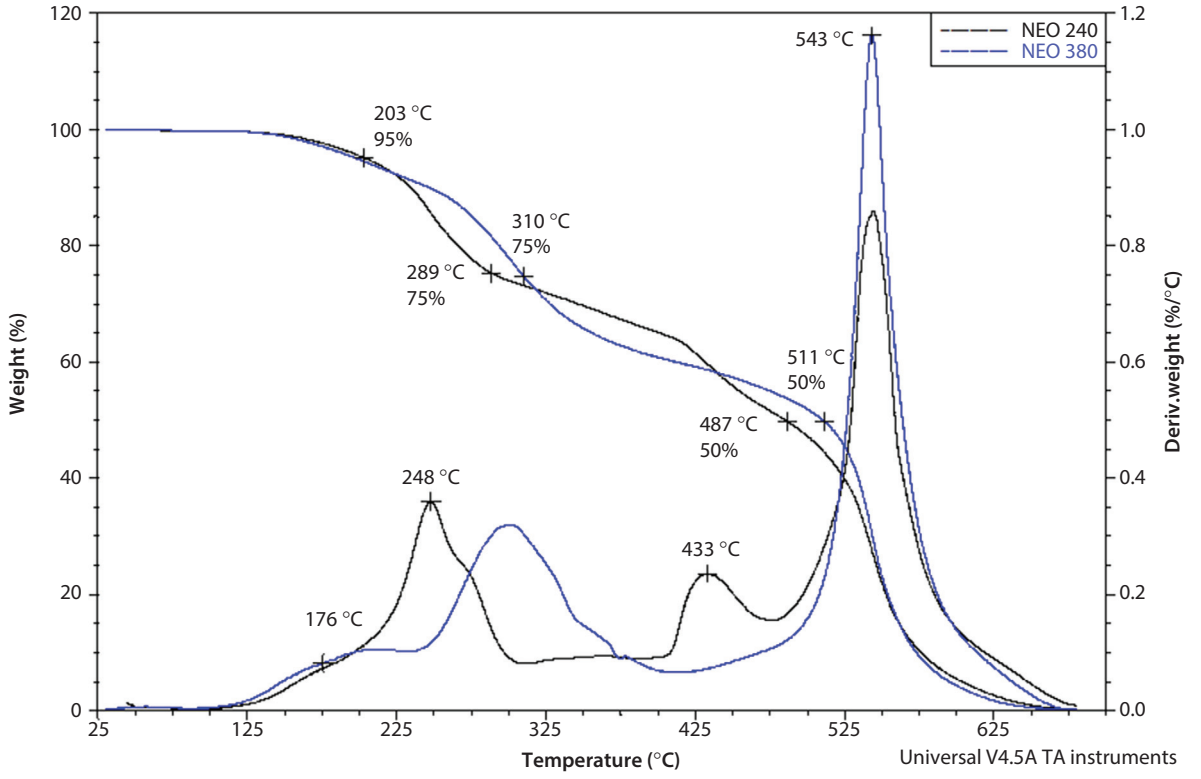

Figure 9 TGA curves for PU foams from Neo 240 and Neo 380 polyols.

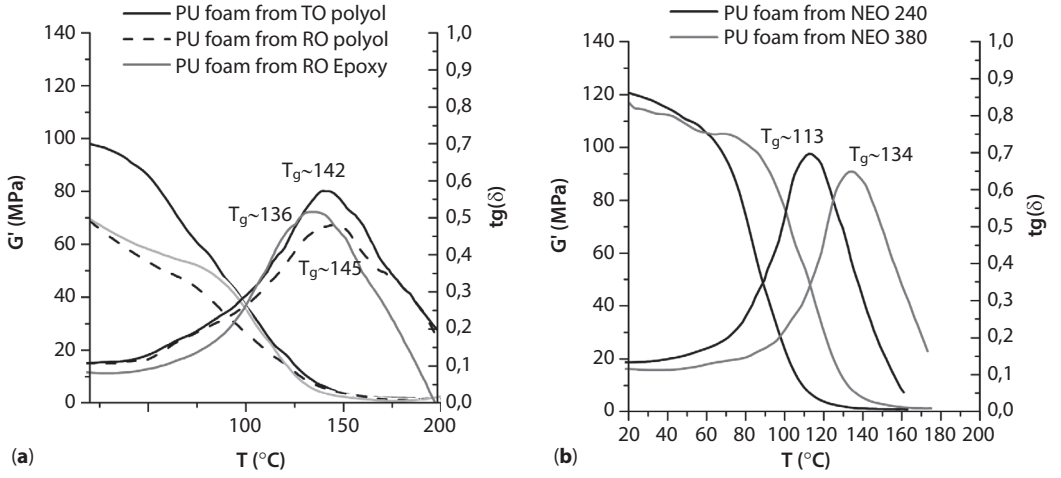

Figure 10 DMA curves for PU foams from different polyols: (**a**) renewable polyols; (**b**) recycled polyols.

properties in the desired exploitation temperature range and are suitable as the core material for sandwich panels [30–43].

3.5 FTIR Analysis of PU Foams

The chemical structure of the developed rigid PU foam materials was confirmed by FTIR analysis. Figure 11 shows FTIR spectra for PU foams from TO polyol RO Epoxy polyol and recycled PET – Neo 380 polyol. Signals in the range of 3337–3330 cm^{-1} are the result of symmetric and asymmetric stretching vibrations of the N-H groups present in urethane groups. At 2924 cm^{-1} and 2854–2852 cm^{-1}, symmetric and asymmetric CH_2 stretching vibrations are observed, which are assigned to the flexible segments of the PU matrix. The next peak

 © 2016 Scrivener Publishing LLC

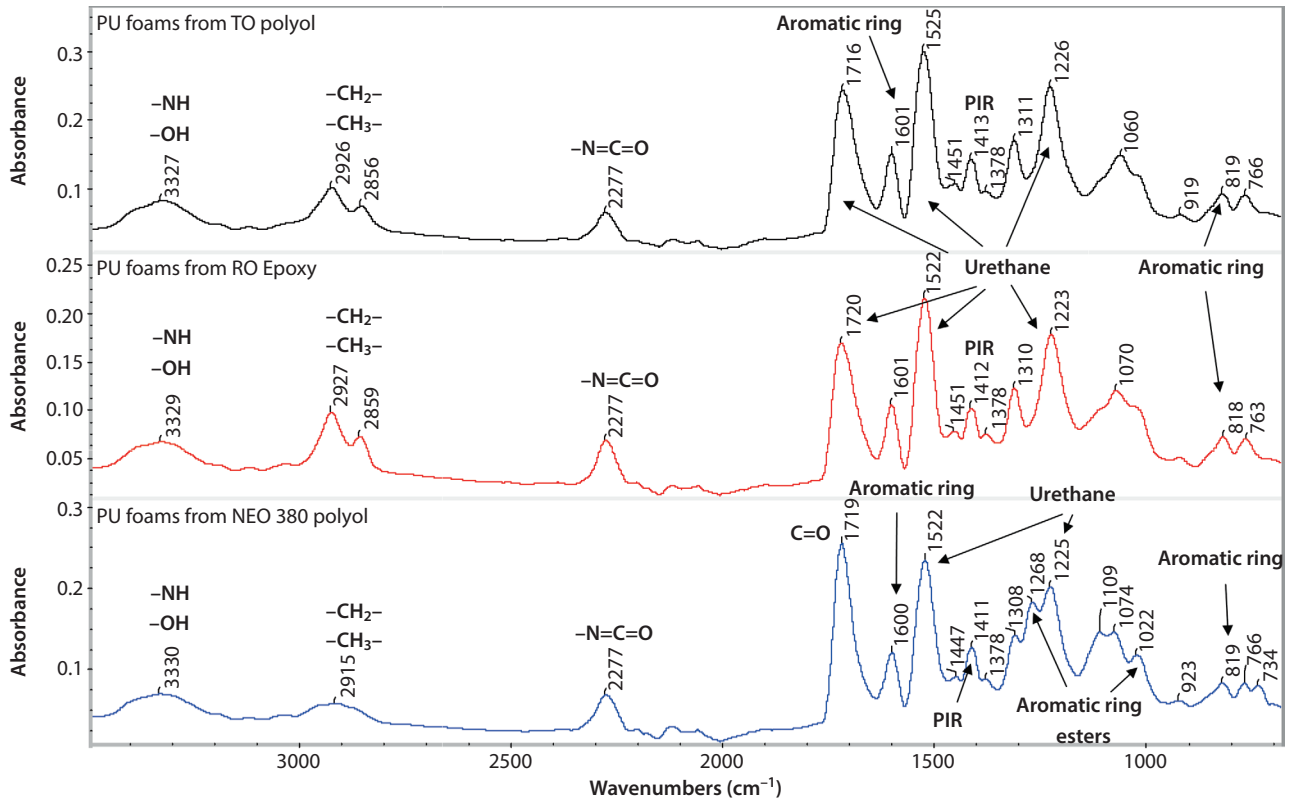

Figure 11 FTIR spectra for rigid PU foams from TO, RO and RO Epoxy polyols.

of the NCO group stretch at 2280 cm^{-1} is attributed to traces of unreacted isocyanate. The C=O stretch at 1723–1714 cm^{-1} is attributed to urethane and urea groups as well as carboxyl groups of the used polyols. There is a distinct peak of aromatic groups at ~1595 cm^{-1} and a peak of trimerization products of isocyanate at 1410 cm^{-1}. the peaks at ~1520 cm^{-1} and ~1310 cm^{-1} are attributed to the in-plane N-H bending and NCO stretching of the urethane group. For PU foams obtained from APP polyols, aromatic acid esters' C-O-C stretching at ~ 1270 and ~ 1103 cm^{-1} was detected [30].

The analysis of the constituent bands of the multiplet band in the range of 1760–1650 cm^{-1} can be seen in Figure 12. The deconvolution of this peak permitted calculating the participation of urethane (U_1), urea (U_2) and allophanate (A_L) bonds in hard segments, as well as the degree of phase separation (DPS). Results for all five PU foams from renewable and recycled polyols are presented in Table 6.

The multiplet bond consists of bonds originating from the C=O group vibrations of urea bond, where hydrogen bonded at 1686–1640 cm^{-1} and unbonded at 1702–1690 cm^{-1}; and from the C=O groups vibrations of urethane bond, hydrogen bonded at 1727–1705 cm^{-1} and unbonded at 1760–1736 cm^{-1}, as well as from allophanate groups vibrations at 1760–1750 cm^{-1} [23, 30, 35–38].

FTIR spectra analysis showed that rigid PU foams had high urea group content compared to other PU materials, due to the blowing agent used—water [30]. PU foams from PET polyols had a higher content of hydrogen-bonded urethane groups than PU foams from renewable polyols. This is because the carbonyl absorption region of the hydrogen-bonded urethane group also contained signals of aromatic esters of PET (1730–1715 cm^{-1}). In all PU foams, allophanate bonds were only marginally present.

4 CONCLUSIONS

This study has shown that polyols from renewable and recycled resources are a viable option for production of high-density rigid PU foams. PU foams with renewable material content up to 19% and an apparent density of 200 ± 10 kg/m^3 were obtained. It has been found that TO and rapeseed oil polyols are a viable counterpart to recycled PET polyols, although their mechanical characteristics are slightly worse. PET polyols allowed obtaining PU foams with a smaller cell size and a more even cell size distribution. TGA analysis showed that the RO epoxy polyol and PET polyols had a higher thermal stability, but all types of PU foams had much higher

© 2016 Scrivener Publishing LLC

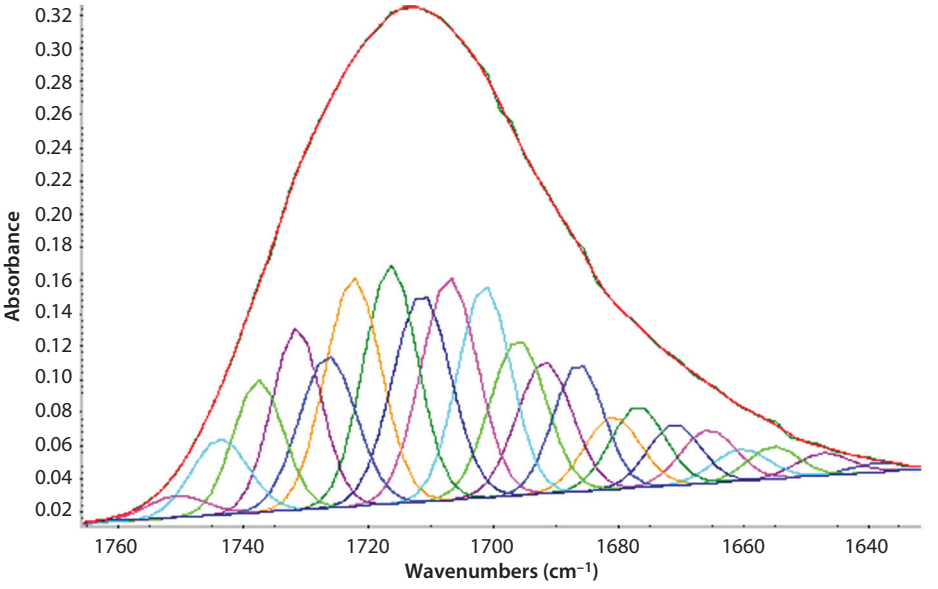

Figure 12 Carbonyl group stretching band of the multiplet structure in the FT-IR spectrum of PU foam from Neo 380 and peaks after the curve-fitting process.

Table 6 Hydrogen bond index ($R_{C=O}$), degree of phase separation (DPS) and PU foam hydrogen bonded urethane (U_1) and urea (U_2) and alaphonate (A_L) group content.

Polyol type	U_1, %	U_2, %	A_L, %	$R_{C=O}$	DPS, %
TO polyol	23	41	0.3	2.21	69
RO polyol	21	40	0.1	2.92	75
RO epoxy polyol	20	43	1	1.54	61
NEO 240	18	53	0.2	2.41	71
NEO 380	19	48	0.53	2.57	71

T_g than the desired range for materials' exploitation. However, DMA test results showed that PU foams from renewable polyols had less stable and repeatable properties.

The chemical structure of the obtained materials was investigated using FTIR spectroscopy. The developed PU foams contained unreacted isocyanate and polyol components. For total conversion of raw materials, other catalytic system and curing parameters should be investigated. Analysis of hydrogen-bonded urethane and urea groups in PU foams allowed establishing the degree of phase separation. Results have shown that almost 70% of hard segments in the PU material are connected together with hydrogen bonds.

This study was done as part of the EU FP7 project EVolution, whose goal is to develop sustainable materials for automotive application. High-density rigid PU foams could be used as core material for crash absorption. In the framework of this project, the desired application would be as impact absorption material used to fill PP crash boxes and crash beams of vehicles.

ACKNOWLEDGMENT

The research leading to these results has received funding from the EC 7th FP project EVolution under the grant agreement n° 314744.

REFERENCES

1. F. Seniha Güner, Y. Yağcı, and A.T. Erciyes, Polymers from triglyceride oils. *Prog. Polym. Sci.* **31**(7), 633–670 (2006).
2. L. Montero de Espinosa and M.A.R. Meier, Plant oils: The perfect renewable resource for polymer science?! *Eur. Polym. J.* **47**, 837–852 (2011).
3. M.A. Mosiewicki and M.I. Aranguren, A short review on novel biocomposites based on plant oil precursors. *Eur. Polym. J.* **49**(6), 1243–1256 (2013).

© 2016 Scrivener Publishing LLC

4. J.M. Raquez, M. Deléglise, M.F. Lacrampe, and P. Krawczak, Thermosetting (bio) materials derived from renewable resources: A critical review. *Prog. Polym. Sci.* **35**(4), 487–509 (2010).
5. M. Ionescu, *Chemistry and Technology of Polyols for Polyurethanes*, pp. 1–586, Smithers Rapra Publishing, Shawbury (2005).
6. C. Scrimgeour, Chemistry of Fatty Acids. *Bailey's Industrial Oil and Fat Products. 1:1*, pp. 1–43, John Wiley & Sons, New York (2005).
7. Z.S. Petrovič, Polyurethanes from vegetable oils. *Polym. Rev.* **48**, 109–155 (2008).
8. U. Stirna, A. Fridrihsone, M. Misane, and D. Vilsone, Rapeseed oil as renewable resource for polyol synthesis. *Scientific Journal of Riga Technical University* **6**, 85–90 (2011).
9. M. Kirpluks, U. Cābulis, M. Kurańska, and A. Prociak, Three different approaches for polyol synthesis from rapeseed oil. *Key Eng. Mat.* **559**, 69–74 (2013).
10. M. Kurańska, P. Aleksander, K. Mikelis, and C. Ugis, Porous polyurethane composites based on biocomponents. *Compos. Sci. Technol.* **75**, 70–76 (2013).
11. M. Kacperski and T. Spychaj, Rigid polyurethane foams with poly(ethylene terephthalate)/triethanolamine recycling products. *Polym. Advan. Technol.* **10**(10), 620–624 (1999).
12. I. Vitkauskienė and R. Makuška, Glycolysis of industrial poly (ethylene terephthalate) waste directed to bis (hydroxyethylene) terephthalate and aromatic polyester polyols. *Chemija* **19**(2), 29–34 (2008).
13. I. Vitkauskienė, R. Makuška, U. Stirna, and U. Cabulis, Thermal properties of polyurethane-polyisocyanurate foams based on poly (ethylene terephthalate) waste. *Materials Science Medžiagotyra* **17(**3), 249-253 (2011).
14. Nasdaq, Crude oil markets, http://www.nasdaq.com/markets/crude-oil.aspx?timeframe=10y (2015).
15. R.K. Helling and D. Russell, Use of life cycle assessment to characterize the environmental impacts of polyol production options. *Green Chem.* **11**(3), 380–389 (2009).
16. Elmira, Bio Polymers and Bio PrePregs Supplier, http://elmira.co.uk/ (2015).
17. Basf, Products and Industry, Lupranol Balance 50, https://www.basf.com/en/company/sustainability/management-and-instruments/quantifying-sustainability/eco-efficiency-analysis/examples/lupranol-balance-50.html (2015).
18. Cargill, BiOH polyols and polymers, http://www.cargill.com/products/industrial/foam/ (2015).
19. K. Hill, Fats and oils as oleochemical raw materials. *Pure Appl. Chem.* **72**(7), 1255–1264 (2000).
20. S.N. Naik, V.V. Goud, P.K. Rout, and A.K. Dalai, Production of first and second generation biofuels: A comprehensive review. *Renew. Sust. Energ. Rev.* **14**(2), 578–597 (2010).
21. R.E.H. Sims, W. Mabee, J.N. Saddler, and M. Taylor, An overview of second generation biofuel technologies. *Bioresource Technol.* **101**(6), 1570–1580 (2010).
22. U. Cabulis, M. Kirpluks, U. Stirna, M.J. Lopez, and M.C. Vargas-garcia, Rigid polyurethane foams obtained from tall oil and filled with natural fibers: Application as a support for immobilization of lignin-degrading microorganisms. *J. Cell. Plast.* **48**(6), 500–515 (2012).
23. K. Pietrzak, M. Kirpluks, U. Cabulis, and J. Ryszkowska, Effect of the addition of tall oil-based polyols on the thermal and mechanical properties of ureaurethane elastomers. *Polym. Degrad. Stabil.* **108**, 201–211 (2014).
24. A. Demirbas, Methylation of wood fatty and resin acids for production of biodiesel. *Fuel* **90**(6), 2273–2279 (2011).
25. F. Balo, Feasibility study of 'green' insulation materials including tall oil: Environmental, economical and thermal properties. *Energ. Buildings.* **86**, 161–175 (2014).
26. A. Austin, Global overview of the PU industry: Prospects & possibilities, *Proceedings of International Conference UTECH'2006*, CD-rom (2006).
27. R. Peacock, Reviewed and revised - the global polyurethane industry 2005 – 2012: future prospects in an uncertain world, *Proceedings of International Conference UTECH'2009*, CD-Rom (2009).
28. M.J. Elwell, H. Kawabata, H. Kramer, D.D. Latham, C.A. Martin, B.C. Obi, V. Parenti, A.K. Schrock, and R. van den Bosch, Polymeric foams: Mechanisms and materials. *Rigid Polyurethane Foams* 1–360 (2004).
29. M.C. Hawkins, Cell morphology and mechanical properties of rigid polyurethane foam. *J. Cell. Plast.* **41**(3), 267–285 (2005).
30. M. Zieleniewska, M. Auguścik, A. Prociak, P. Rojek, and J. Ryszkowska, Polyurethane-urea substrates from rapeseed oil-based polyol for bone tissue cultures intended for application in tissue engineering. *Polym. Degrad. Stabil.* **108**, 241–249 (2014).
31. Neo Group, products, http://neopolyol.eu/products (2015).
32. S. Vijayakumar and P.R. Rajakumar, Infrared spectral analysis of waste pet samples. *Int. Lett. Chem. Phys. Astron.* **4**, 58–65 (2012).
33. E. Žagar and J. Grdadolnik, An infrared spectroscopic study of H-bond network in hyperbranched polyester polyol. *J. Mol. Struct.* **658**(3), 143–152 (2003).
34. Z. Xing, G. Wu, S. Huang, S. Chen, and H. Zeng, Preparation of microcellular cross-linked polyethylene foams by a radiation and supercritical carbon dioxide approach. *J. Supercrit. Fluid.* **47**(2), 281–289 (2008).
35. J. Ryszkowska, Supermolecular structure, morphology and physical properties of urea-urethane elastomers. *Polimery* **57**, 777–785 (2012).
36. M. Zieleniewska, M. Auguścik, A. Prociak, P. Rojek, and J. Ryszkowska, Polyurethane-urea substrates from rapeseed oil-based polyol for bone tissue cultures intended for application in tissue engineering. *Polym. Degrad. Stab.* **108**, 241–249 (2014).
37. T. Pretsch, I. Jakob, and W. Müller, Hydrolytic degradation and functional stability of a segmented shape memory poly(ester urethane). *Polym. Degrad. Stabil.* **94**(1), 61–73 (2009).
38. Y.I. Tien and K.H. Wei, Hydrogen bonding and mechanical properties in segmented montmorillonite/polyurethane nanocomposites of different hard segment ratios. *Polymer.* **42**, 3213–3221 (2001).

© 2016 Scrivener Publishing LLC

39. J.L. Ryszkowska, M. Augus´cik, A. Sheikh, and A.R. Boccaccini, Biodegradable polyurethane composite scaffolds containing Bioglass® for bone tissue engineering. *Compos. Sci. Technol*. **70**(13), 1894–1908 (2010).
40. L. Jiao, H. Xiao, Q. Wang, and J. Sun, Thermal degradation characteristics of rigid polyurethane foam and the volatile products analysis with TG-FTIR-MS. *Polym. Degrad. Stabil*. **98**(12), 2687–2696 (2013).
41. D.K. Chattopadhyay and D.C. Webster, Thermal stability and flame retardancy of polyurethanes. *Prog. Polym. Sci*. **34**(10), 1068–1133 (2009).
42. A. Fridrihsone-Girone and U. Stirna, Characterization of polyurethane networks based on rapeseed oil derived polyol. *Polimery/Polymers* **59**, 333–338 (2014).
43. L. Wu, J. Van Gemert, and R.E. Camargo, Rheology study in polyurethane rigid foams, Huntsman Corporation Technical Paper.

© 2016 Scrivener Publishing LLC